THREE-DIMENSIONAL RECONSTRUCTIONS OF THE DOLPHIN EAR

Darlene R. Ketten[1] and Douglas Wartzok[2]

[1]Department of Otology and Laryngology
Harvard Medical School, Boston, Massachusetts, USA
[2]Department of Biological Sciences
Purdue University, Fort Wayne, Indiana, USA

INTRODUCTION

The umwelt or perceptual world of odontocetes is largely defined by acoustic cues imperceptible to humans. Like bats, they use ultrasonic frequencies to echolocate. To penetrate this acoustic world, we must use indirect anatomical and psychophysical techniques. While bat research has incorporated anatomy and physiology to describe neural processing of echolocation signals, cetacean research, hampered by practical and legal restrictions, depends largely upon spectral and temporal analyses of emitted sounds coupled with behavioral observations. From these investigations, we have gained considerable information about the psycho-acoustics of dolphin echolocation, but we still know little about the receptor anatomy.

This study is based on an anatomical comparison of inner ear structure in twelve species. A comparative anatomy approach was chosen for two reasons. First, peripheral auditory structures are important components in determining hearing capacities (West, 1986; Stinson, 1983; Zwislocki, 1981; Iurato, 1962). Secondly, it is more feasible to obtain adequately preserved cochlea for most odontocetes than central nervous system tissues. In bats, ultrasonic vocalization spectra and auditory sensitivity are directly related and anatomical correlates for frequency ranges are well documented (Suga, 1983; Long, 1980; Neuweiler, 1980; Pollack, 1980; Bruns; 1976; Sales and Pye, 1974; Hinchcliffe and Pye, 1968; Grinnell, 1963). Electrophysiological recordings and neuroanatomical studies from Tursiops and Stenella show similar structural correlates for emitted signals (Ridgway, 1980; Bullock and Ridgway, 1972; McCormick et al., 1970; Bullock et al., 1968). All odontocetes recorded to date produce ultrasonics in species-specific frequency ranges and are assumed to echolocate (Watkins and Wartzok, 1985; Pilleri, 1983; Popper, 1980; Wood and Evans, 1980; Norris et al., 1961; Kellogg, 1959). Thus, we expect extreme differences in echolocation signals to reflect anatomical differences in the auditory periphery. Three-dimensional reconstructions in this study of odontocete cochlea show structural similarities between bat and odontocete inner ears related to ultrasonic perception and

Sensory Abilities of Cetaceans
Edited by J. Thomas and R. Kastelein
Plenum Press, New York, 1990

interspecific differences amongst odontocetes which correlate with echolocation ranges. These analyses also show specific adaptations of the dolphin ear for aquatic audition.

METHODS

Any investigation of cetacean sensory systems must consider practical and legal limitations. Live research implies the obvious difficulties of maintaining large aquatic animals and meeting Marine Mammal Protection Act strictures. Acute preparation studies are restricted and require exceptional skills and facilities (Ridgway et al., 1974; Ridgway and McCormick, 1967; Nagel et al., 1964). Access to animals in commercial facilities is limited and many captive animals have been treated with preventative antibiotic regimens which may include ototoxic agents (Montali and Migaki, 1980). Most morphometric studies of cetacean bullae use dehydrated or unpreserved tissues collected days to weeks post-mortem (Norris and Leatherwood, 1981; Fleischer, 1976; Kasuya, 1973; Fraser and Purves, 1960). An approach was needed that obviated the physiological, mechanical, and political problems of live animal research yet would yield more than standard morphometric detail. In contrast to the availability of live animals, substantial numbers of cetaceans are netted or stranded annually in fisheries and well-preserved material is archived worldwide. By developing collection and analysis techniques applicable to these tissues, the data base could be significantly increased in terms of both individuals and total species examined.

Key species were determined prior to collection for this research since distribution of specimens by species, functional diversity, and quality of tissue was crucial. Selection criteria included ultrasonic frequency spectra, taxonomic relationships, habitat, degrees of sociality, and feeding strategies. Sixty-three bullae were obtained through a specimen request survey, of which fifty-five were accepted for complete analyses (Table 1). Key species covered four odontocete families which represent different eras of collateral development and several degrees of specialization for the major evolutionary divisions of extant species (Kasuya, 1973). Habitats ranged from estuarine through sublittoral and pelagic to transitional bathypelagic for deep-diving species. Bullae from opportunistic (non-key) species of exceptional quality were analyzed by the same procedures as key specimens. Measurements from opportunistic specimens were used in family analyses, but, without conspecifics for comparison, were not considered adequate for species analyses. All tissues came from four sources: (1) bullae from fisheries or aboriginal hunts extracted and preserved in situ in buffered formalin; (2) bullae extracted and injected with buffered formalin or glutaraldehyde during necropsy; (3) whole heads or temporal blocks preserved on dry ice and thawed in buffered formalin; (4) perfused, archival animals analyzed only with radiography and returned to the lending facility.

Acoustic data for key and related species are listed in Table 2. A major concern in this study was to find a reliable measure of hearing for each species. Odontocetes have a wide functional range, but underwater auditory selectivity and sensitivity measures are available for very few species. Like most mammals, however, cetaceans produce sounds centered around frequencies at which their hearing is most acute. Lower frequency communication signals, as defined in Popper (1980), vary greatly with individuals and have little or no species-

Table 1. Specimen Distributions

Classification	Common name	Bullae	Left	Right	Male	Female
Suborder ODONTOCETI		57	31	26	19	15
Family DELPHINIDAE		39	21	18	9	13
Delphinus delphis	common dolphin	2	1	1	1	
Feresa attenuata	pygmy killer whale	2	1	1	1	
Globicephala macrorhynchus	short-finned pilot whale	2	1	1	1	
Grampus griseus†	Risso's dolphin	4	2	2	1	1
Lagenorhynchus albirostris†	White-beaked dolphin	3	2	1		3
Stenella attenuata†	spotted dolphin	16	8	8	1	7
Stenella coeruleoalba	striped dolphin	2	2		1	1
Stenella longirostris	long-beaked spinner	2	1	1	1	
Tursiops truncatus†	bottlenose dolphin	6	3	3	2	1
MONODONTIDAE						
Monodon monoceros	narwhal	2	1	1	1	
PHOCOENIDAE						
Phocoena phocoena†	harbour porpoise	8	4	4	2	2
PHYSETERIDAE						
Physeter catodon††	sperm whale	6	4	2	6	
PLATANISTIDAE						
Inia geoffrensis††	Amazonian boutu	2	1	1	1	

† Key species

†† Key specimens examined only with radiography

specifity. Echolocating animals vary pulse repetition rate, interpulse interval, intensity, and click spectra and it is known that captive animals selectively modify echolocation pulses in response to ambient noise (Moore, 1990; Supin and Popov, 1990; Thomas et al., 1988; Popper, 1980; Au et al., 1974; Norris, 1969; Schevill, 1964). Nevertheless, echolocation signals tend to be produced in species-specific frequency ranges. Echolocation signals, from which ultrasonic auditory ranges can be inferred, provide the most consistent comparative acoustic data for all species in this study. Species were categorized into two groups based on the peak spectra of their echolocation signal; i.e., the frequency of maximum energy in a typical, broadband echolocation click. Data from recordings of untrained animals in natural surroundings were used when available. Specimens from species with a peak signal energy located above 100 kHz, Phocoena phocoena and Inia geoffrensis, were designated Group I (Table 2). Those from species with ultrasonic peak spectra below 100 kHz comprised Group II. For some species, little or no acoustic data are available and they are subsequently categorized based on cochlear morphometry.

Table 2. Characteristics of Odontocete Sounds
(Adapted with permission from Popper, 1980)

Acoustic Group and Species	Type of sound	Frequency Range (kHz)	Maximum Energy (kHz)	References
I				
Inia geoffrensis	Click	25-200	100	Norris et al., 1972
			95-105	Kamminga et al., 1989
Phocoena phocoena	Pulse	100-160	110-150	Møhl and Andersen, 1973
II				
Delphinus delphis	Click		4-9	Busnel and Dziedzic, 1966
	Whistle	4-16		Gurevick in Evans, 1973
	Click	0.2-150	30-60	Gurevick in Evans, 1973
Lagenorhynchus	Click	0.06-80		Evans, 1973
obliquidens	Whistle	1-12		Caldwell and Caldwell, 1971
Stenella attenuata	Pulse	to 150		Diercks, 1972
	Whistle			Evans, 1967
Stenella longirostris	Click	.1-160	60	Ketten, 1984
	Pulse	1-160	5-60	Brownlee, 1983
	Whistle	1-20	8-12	Brownlee, 1983
Tursiops truncatus	Click	>octave	53†	Diercks et al., 1971
	Click	0.2-150	30-60	Diercks et al., 1971
	Bark	0.2-16		Evans, 1973
	Whistle	4-20		Evans and Prescott,1962
	Whistle	2-20		Caldwell and Caldwell, 1967
Unknown††				
Physeter catodon	Coda	16-30		Watkins and Schevill, 1977
Grampus griseus	Whistle			Watkins and Wartzok,1985

† Au et al. (1974) reported clicks by trained animals in noise with 100-130 kHz spectra.
†† No wide band recordings are available for these species.

All specimens were screened by one or more of three radiographic techniques: single plane stereo-radiography, digital subtraction, and computerized tomography (CT scanning). The principal advantage of radiography for surveying cochlea is that it provides non-destructive techniques for viewing structures in situ (Fig. 1). CT also provides a numerical data base for quantitative analyses and, through multiplanar image reconstruction, a "dissection" of the cochlea without extraction or decalcification. CT scans were obtained with a Siemens Somatom DR3 in the Johns Hopkins Medical Institutions. The DR3 scanner generates parallel, contiguous transaxial slices of 1 to 8 mm thickness with an optimal resolution of 300μ. Like conventional radiography, CT measures tissue absorption of X-rays. Resolution depends upon the number of exposures, collimators, and detectors; the storage and manipulation capacity of associated computers; and the resolution of the image display. The mammalian cochlea, comprised of bone, soft tissue, and fluid, is an ideal subject for CT examination since optimal CT resolution occurs at interfaces of high and low density tissue (Maue-Dickson et al., 1983; Moran et al.,1983). Densest bone in normal humans

measures <2000 H.U.[1], but in cetaceans, the temporal bone may exceed 3000 H.U.. This density allows exceptional cross-sectional imaging of both bony and residual soft tissues in odontocete bullae (Fig. 2). Scan parameters used in this survey were 90-100 kV accelerating voltage, 0.5-0.6 milliamp-seconds (MAS), 720 projections, 1-2 mm slices, 512 matrix high resolution imaging, and a 0.3 m image aperture. Data and images were stored on disk and magnetic tape as raw absorption data, cross-sectional images, and reconstructions.

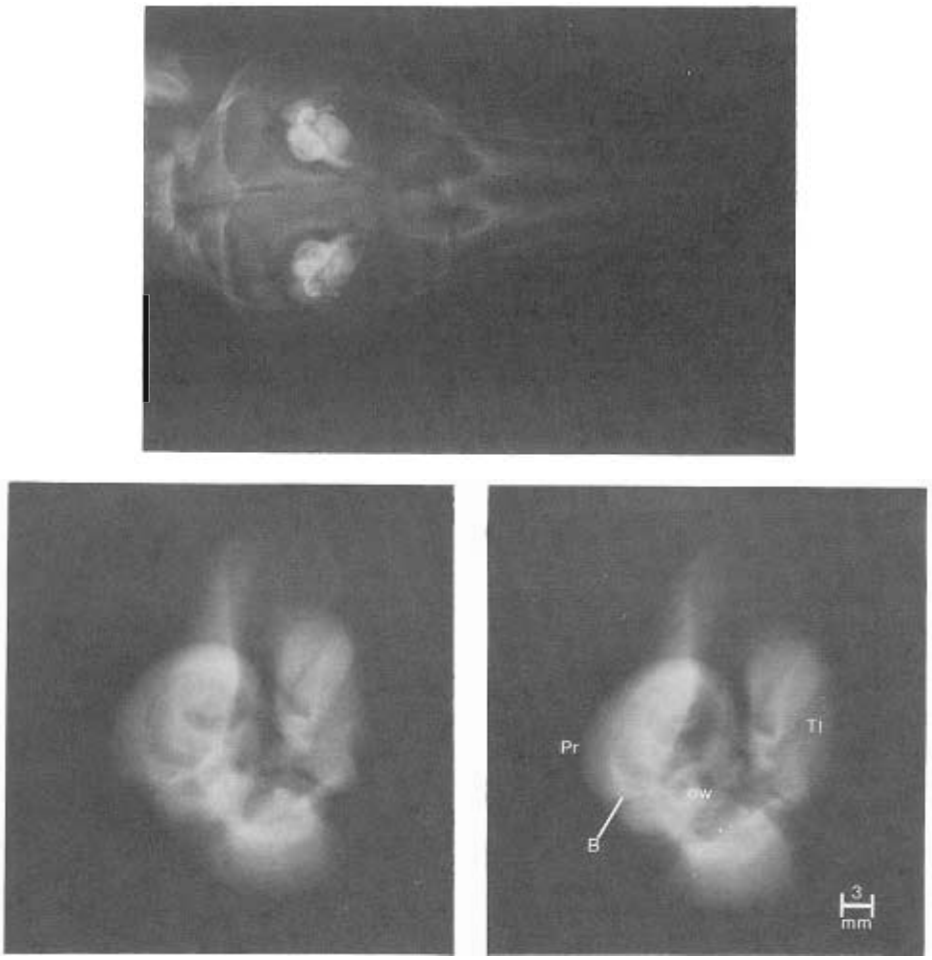

Fig. 1. Stereoradiography of Odontocete Ears. A single plane X-ray of a juvenile Stenella attenuata head and stereo-paired images of the right bulla show the cochlea in the promontorium (Pr) of the periotic medial to the less dense tympanic lobe (Tl). Radiographs image structures in a grayscale proportional to X-ray attenuation, from white for densest material to black for air. The high contrast of the bullae results from their exceptional tissue density. The basal turn of the cochlea (B) can be seen curving posteriorly and medially from the oval window (ow) in each ear.

[1]Hounsfield Units, derived from the linear attenuation coefficient of a substance normalized to water, provide a relative measure of tissue density or X-ray absorption characteristics in a range of -1000 (air) to <+4200 (metal).

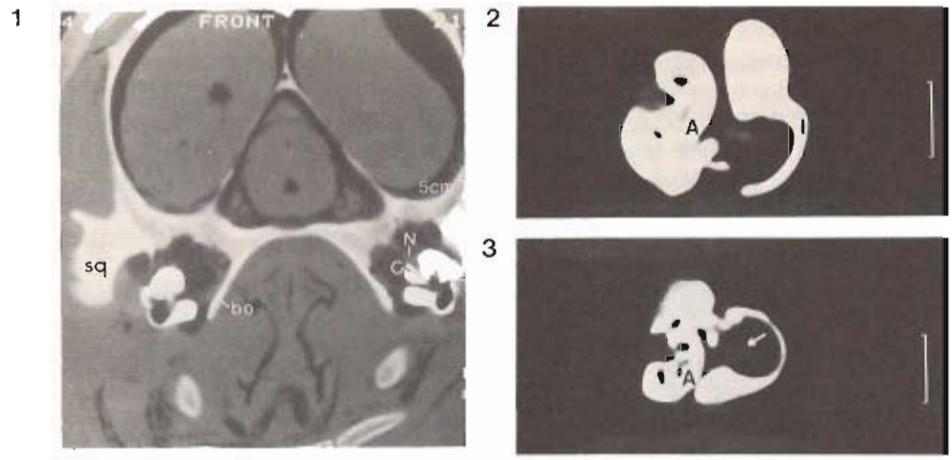

Fig. 2. CT Scans of Cochlear Anatomy. (2.1) A transaxial CT scan of an adult Tursiops truncatus head shows the relationship of the bulla to major cranial structures. The peribullar cavity is ventral to the cerebral hemispheres and is bordered by the ventrolateral process of the basioccipital (bo) and the squamosal (sq) bones. Suspensory ligaments in the cavity are gray as is the auditory nerve (N), which enters the periotic via the internal auditory canal and is flanked by cross-sections of the cochlear spiral (C). The hollow mandible (Ma) is ventral to the tympanic bulla. On the right, high contrast, magnified scans show the cochlea in cross-section in (2.2) Phocoena (1.5 turns) and (2.3) Stenella (2.5 turns). Gray bands of soft tissue in the tympanic cavity (arrow) are folds of the corpus cavernosum. Scale bars represent 1 cm. A apex; l lateral.

After scanning, bullae were extracted, cleaned, weighed, catalogued, and measured. For key species, the periotic was decalcified, embedded in paraffin or celloidin, and examined in 20 μ serial sections. Four methods of decalcification were attempted; a formic acid and formalin-based modification of Schmorl's solution provided the best balance of efficacy vs. distortion. Three to four fiducials were used to gauge processing artifacts and for alignment of reconstructions. Histological procedures are detailed in Ketten (1984).

Cochlear canal midpoints and anatomical contours were digitized from CT images and histological sections to obtain Cartesian triplets (X,Y,Z) for three-dimensional mapping, measurement, and reconstruction of the cochlear duct. Approximately 30 mid-canal triplets, progressing from the stapes to the helicotrema, were used to map the cochlea and to calculate spiral dimensions for each specimen. Contour coordinates were used to reconstruct cochlear duct and bullar components and to calculate exterior surface area and volume. The SAS statistical package was used for univariate and multivariate statistical analyses of spiral and bullar measurements. Left and right bullae were treated as individual entries to test for asymmetry. Statistical analyses were performed on both raw data and on values normalized by animal length for interspecific comparisons.

RESULTS

Bullar Morphometry

The bulla or temporal bone of odontocetes is distinctive and dense. It differs from terrestrial mammalian bullae in appearance, construction, location, orientation, and, in some aspects, function. It is not fused to the skull as in other mammals but is suspended by ligaments in a peribullar cavity with the long axis of the tympanic angled ventromedially (Figs. 1,2). The periotic is dorsal to the tympanic and the shorter, vertical bullar axis is rotated medially 15° to 20°. The acousto-vestibular (VIIIth) nerve projects inward from the dorsomedial edge of the periotic, traverses the retro-peribullar space, and enters a dense, bony canal. The periotic is relatively uniform in thickness, composed of compact bone, and encloses the cochlea, vestibule, and the residual components of the vestibular apparatus. The tympanic has a thickened posterior; a thin, friable body; and a narrow anterior process. The concha or tympanic shell is lined with a membranous corpus cavernosum and contains the ossicular chain and a partially ossified tympanic conus. In all species except Physeter, a band of fibrous tissue, analogous to the stylo-hyoid ligaments, joins the posterolateral edge of the bulla to the posterior margin of the mandibular ramus and stylo-basihyoid complex. In all whole heads, the right bulla was located anteriorly to the left.

Surface anatomy is resilient in dehydrated specimens and has been carefully assessed in other studies (Oelschlager, 1990, 1986; Kasuya, 1973; Reysenbach de Haan, 1956). All surface measurements in this survey (Table 3) are consistent with previous results and are strongly correlated with animal size ($r \geq 0.9$). Linear discriminant analyses redistributed surface data by species with the smallest squared distances amongst delphinids (1400-32000) and the largest between phocoenids and delphinids (110000-156000). T-tests on normalized data showed no significant differences between Groups I and II. Schematic surface reconstructions (Fig. 3) revealed no clear-cut group characteristics although there are visible differences amongst species in the solidity of the periotic-tympanic

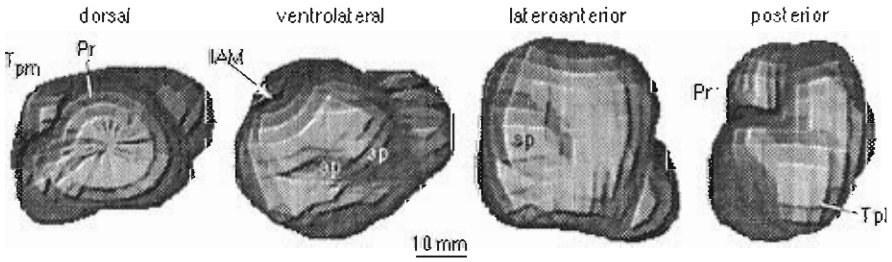

Fig. 3. Solid Surface Reconstructions. CT scans of the right bulla of Tursiops truncatus were digitized, reconstructed, and displayed in four rotations using Multiple Marker Analysis (Graves et al., 1984). Major surface features evident in the reconstruction include the cochlear bulge of the promontorium (Pr), the indentation of the internal auditory meatus (IAM), the petrotympanic aperture (ap) posterior to the sigmoid process (sp), and the lateral (Tpl) and medial (Tpm) posterior tympanic prominences.

Table 3. Bullar Surface Morphometry

Group and Species	Body length (cm)	Bullar Dimensions (mm)[1]	Periotic (mm)[1]	Tympanic (mm)[1]	VIIIth Nerve[2] (mm)	Bullar Weight (gm)	Surface Area[3] (mm^2)	Bullar Volume (ml)[3]
I								
Phocoena phocoena	133	33.2 24.1	30.3 16.3	30.1 19.7	3.7	15.2	2341	9.600
Physeter catodon	1361	69.7 63.9	60.6 36.5	59.6 37.2	11.3	180.7		45.52 (periotic only)
II								
Grampus griseus	228	43.9 32.9	37.3 25.1	38.7 24	4.7	32.7	3190	14.708
Lagenorhynchus albirostris	207	42.2 32.6	30.7 19.0	36.3 22.5	4.6	23.7	2806	12.339
Stenella attenuata	185	33.3 24.7	28.5 19.3	30.9 18.7	4.9	13.3	2341	9.5585
Tursiops truncatus	259	44.0 28.8	31.6 19.8	34.0 21.4	5.5	25.2	2963.7	13.45

[1] Lengths of longest/shortest axes.

[2] Diameter of auditory nerve at the periotic aperture of the internal auditory canal.

[3] Calculated by MMAS from CT scans. There was no significant difference between calculated values and fluid displacement measurements for five test specimens.

suture, the proportions of the bullar divisions, and the complexity and relative position of surface convolutions. Thus, odontocete bullae have species-specific size and shape characteristics which are not correlated with ultrasonic frequency ranges but all are similarly constructed from exceptionally dense, compact bone and are completely isolated from the skull in a peribullar cavity (Fig. 4).

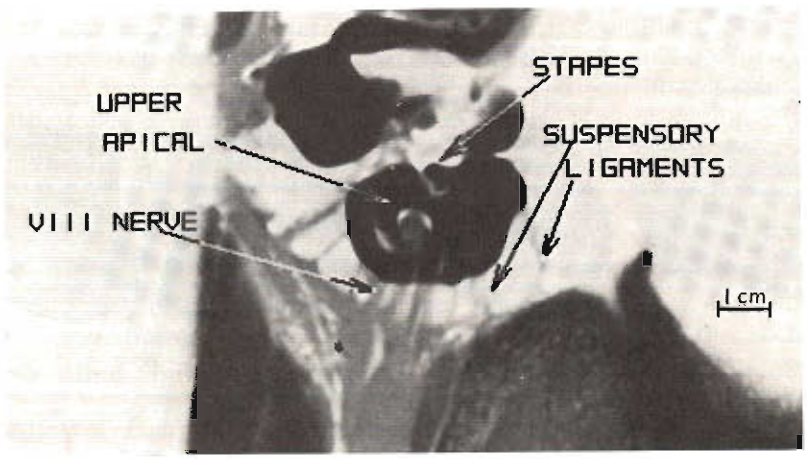

Fig. 4 Sperm Whale Periotic. A 2 mm CT section shows a Physeter catodon bulla from a dorsal view. Five sets of ligaments attach the tympanic and periotic to less dense lamellar bone surrounding the peribullar cavity. Most of the cochlea is visible as it curves for 1.5 turns from the stapes to the apex.

Cytoarchitecture of the Osseus Labyrinth

The dolphin cochlea has the prototypic mammalian divisions: scala media (cochlear duct), scala tympani, and scala vestibuli. The membranous labyrinth of scalae forms an inverted spiral inside the bony labyrinth of the cochlear canal (Fig. 5), which curves medially and ventrally in each periotic from the stapes to the helicotrema at the apex, around a core, the modiolus, containing the auditory branch of the acousto-vestibular nerve. The canal decreases in diameter from base to apex with cross-sectional area ratios ranging 1.6 (Phocoena) to 6.3 (Grampus). In all specimens, the vestibule is large but the semi-circular canals are reduced and

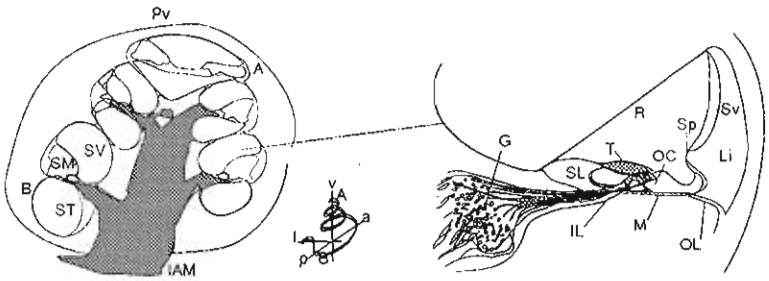

Fig. 5. The Cochlear Canal. Major cochlear structures are shown schematically for a right delphinid ear. On the left, the periotic is bisected along the neural axis in a mid-modiolar plane. It is drawn inverted from in vivo orientation (indicated on the small axes) for comparison with conventional mammalian representations which have the cochlear apex at the top of the image. The light micrographs in Figure 6 are shown in the same orientation. The right enlargement depicts scala media in the mid to upper basal turn, equivalent to the location of Figure 6.1. a anterior, p posterior, l lateral, v ventral; A apex; B basal turn; G spiral ganglia; IAM medial aperture of the internal auditory canal; IL inner spiral lamina; Li spiral ligament; M basilar membrane; OC organ of Corti; OL outer spiral lamina; Pv ventral edge of promontorium; R Reissner's membrane; SL spiral limbus; SM scala media; Sp spiral prominence; ST scala tympani; SV scala vestibuli; Sv stria vascularis; T tectorial membrane.

form incomplete channels; it is unclear whether all components of the vestibular system are functional. All odontocete cochleae examined in thin section differ significantly from other mammalian cochleae (Fig. 6) and structural differences in the basal turn separate odontocetes into two anatomically distinct groups. Three anatomical features of the inner ear which influence resonance characteristics and frequency perception are addressed in detail here: basilar membrane construction, osseous spiral laminae configurations, and spiral ganglion cell distributions.

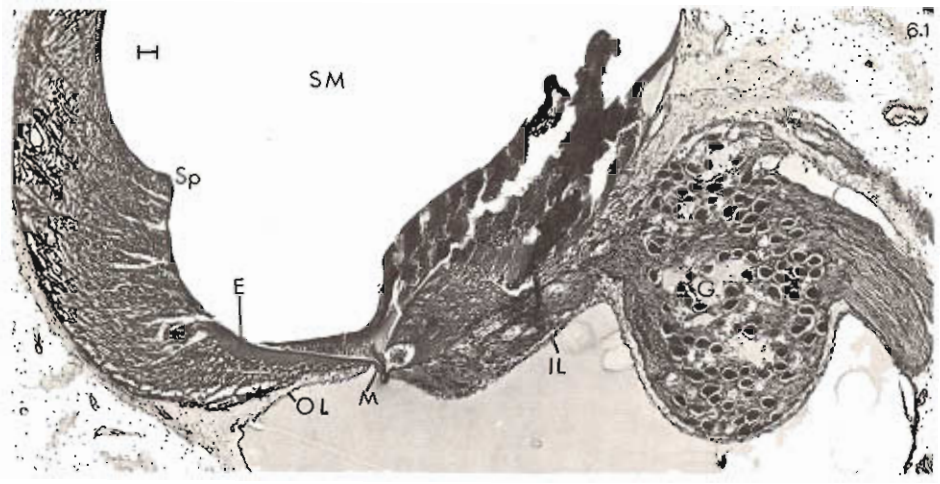

6.1

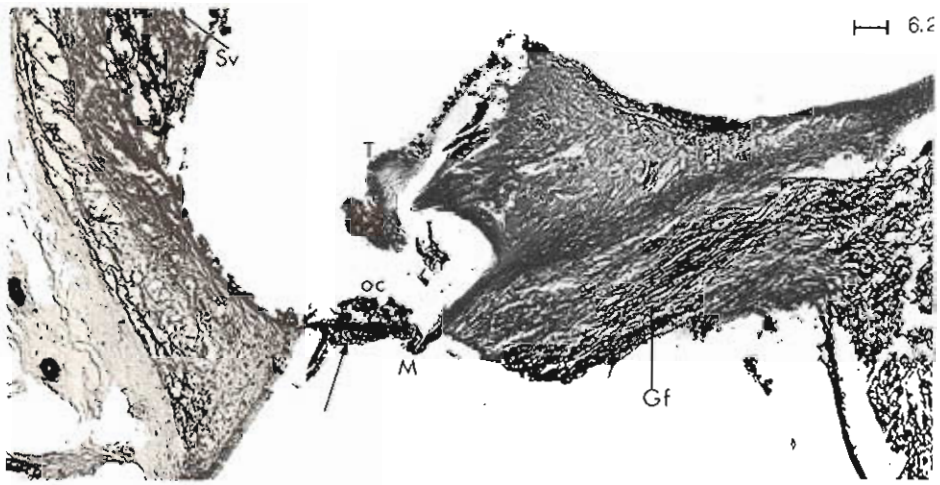

6.2

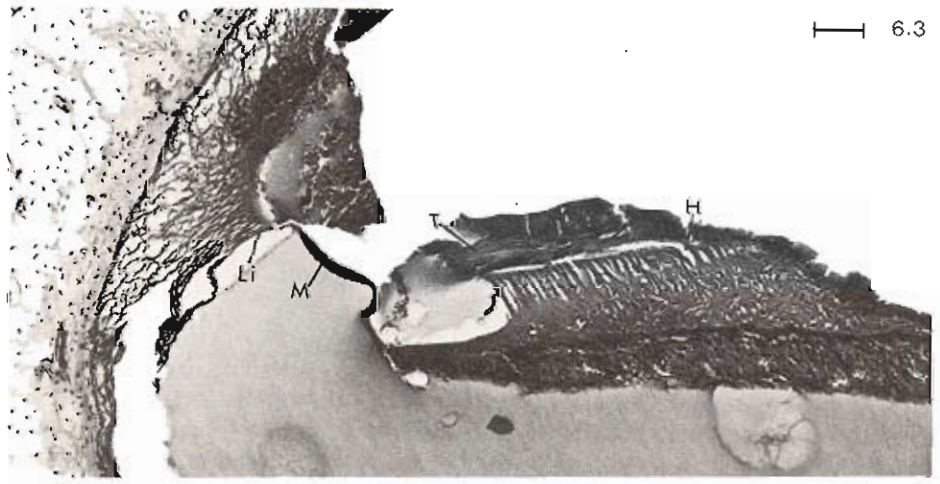

6.3

Fig. 6. Cochlear Duct Cytoarchitecture. Light micrographs of 20 μ mid-modiolar sections demonstrate structural characteristics of the odontocete cochlear duct. Descriptions below use conventional neurocentric orientations for the cochlea in which inner or medial mean towards the modiolus and outer or lateral refer to the anti-modiolar or abneural side of the cochlea. All tissues are from adult animals and represent average material preserved 5 hours to 4 days post-mortem by round window injection. They show preservation and processing artifacts similar to those of human temporal bones, including disruption and collapse of Reissner's membrane, absent or necrotic organ of Corti, acidophilic staining of the perilymph, and serous protein deposits in scala media (SM). Each scale bar represents 50μ .

(6.1.) The basilar membrane (M) of Phocoena phocoena in the upper basal turn, 7 mm from the oval window, measures 45μ x 20μ. It is stretched between inner (IL) and outer (OL) ossified spiral laminae. The outer lamina is is 30-40μ thick. There is heavy staining of the perilymph in scala tympani, but the endolymph of scala media (SM) is not contaminated, indicating the membrane is intact. Blood in scala media is the result of a concussion. A distinctive cellular layer (E) found only in the basal turn in odontocetes lines the lateral basilar membrane recess below the spiral prominence (Sp). Kolmer reportedly dubbed them "ersatzzellen" (Reysenbach de Haan, 1956), and although noted by several authors, these cells are unclassified and their function remains unclear. The large number of oblate spiral ganglion cells (G) clumped medially in a pocket of Rosenthal's canal which protrudes into scala tympani is a typical cross-section of the spiral ganglia in odontocetes.

(6.2) In the upper middle turn of Tursiops truncatus, 28 mm from the stapes, the basilar membrane (190μ x 10μ) is partly obscured by organ of Corti remnants and by mesothelial cells on the tympanic border (arrow). These cells are common in mammals and increase apically. Curvature of the membrane is a compression artifact. The stria vascularis (Sv) is characteristically dense and collagenous. The tectorial membrane (T) extends over the spiral limbus and broadens into a gelatinous flap over the basilar membrane. There is no fibrillar layer analogous to Hensen's stripe in humans. Large numbers of habenular fibers (Gf) are apparent between the inner spiral laminae.

(6.3) In an apical section 4 mm from the helicotrema in Phocoena, the membrane measures 200μ x 10μ. Only the spiral ligament (Li) supports the lateral edge of the basilar membrane at this point. Multiple cells of Huschke (H), the auditory teeth, are visible in the spiral limbus immediately below the limbal tectorial membrane (T).

Basilar membrane thickness and width vary inversely from base to apex in mammals. Highest frequencies are encoded in its narrow, basal region and progressively lower frequencies, towards the apex as the membrane broadens and thins. In all odontocetes, thickness varies uniformly from 25μ basally to 5μ apically with no apparent change in fibrillar density. Width increases 9-12 fold from a basal minimum of 30-40μ (Table 4). Delphinids have a greater increase in membrane width than phocoenids; however, Phocoena phocoena has the steepest rate of increase. Comparisons of bat and odontocete membrane thickness:width ratios (Fig. 7) show parallel slopes for all groups in the lower

Table 4. Basilar Membrane Dimensions

Group and Species	Membrane Length (mm)	Outer Osseous Lamina Length (mm)	Basal/Apical Width (μ)	Basal/Apical Thickness (μ)
I				
Phocoena phocoena	25.93	17.6	30/290	25/5
II				
Grampus griseus	40.5	-	40/420	20/5
Lagenorhynchus albirostris	34.9	8.5	30/360	20/5
Stenella attenuata	36.9	8.35	40/400	20/5
Tursiops truncatus	40.65	10.3	30/380	25/5

frequency apical regions of the cochlea and 2-3 fold higher ratios for odontocetes in the basal ultrasonic regions.

Inner and outer ossified spiral laminae are present throughout most of the basal turn in all species examined and are amongst the most striking features of the odontocete cochlea (Figs. 6,8). The internal osseous spiral laminae, tunneled by the foramina nervosa or nerve fiber tracts, form a bi-layered wedge which supports the medial margin (pars arcuata) of the basilar membrane. The thickness of the inner laminae varies inversely with distance from the stapes. In the lower basal turn, the inner laminar wedge averages 50μ at the membrane juncture. In the middle to upper basal turn it thins to 5μ, and, in delphinids, becomes a single shelf supporting the spiral limbus. The outer lamina in the basal turn in all odontocetes is 30-40 μ thick, heavily calcified, and functions as a housing for the spiral ligament and lateral attachment for the basilar membrane.

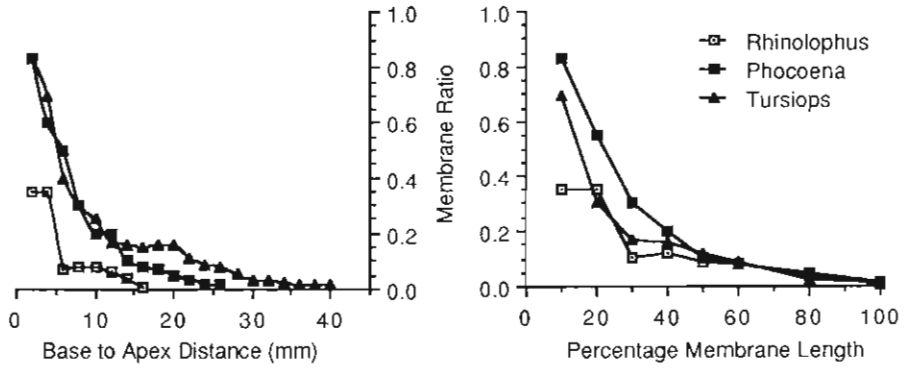

Fig. 7. Basilar Membrane Ratios. Thickness:width ratios for basilar membranes in the horseshoe bat, Rhinolophus ferrumequinum, and two odontocetes (Phocoena phocoena (I); Tursiops truncatus (II)) are plotted against location in the cochlea and as a percentage of cochlear length. The acute decrease in the bat ratio at 5 mm corresponds to a characteristic region of abrupt change in membrane configuration reported in some constant frequency bats associated with the specialized "foveal" membrane region encoding their echolocation signal (Camhi, 1984).

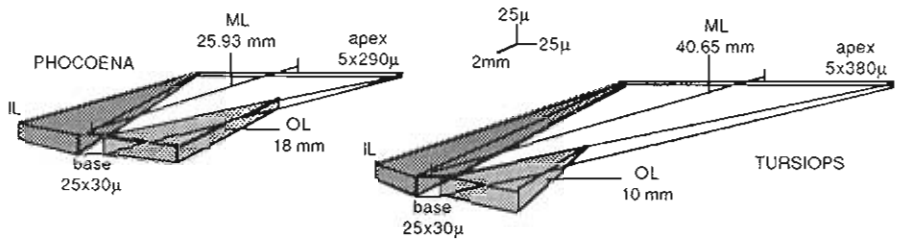

Fig. 8. Laminar Attachments of the Basilar Membrane. The basilar membrane (M) and inner (IL) and outer (OL) osseous spiral laminae are drawn in orthoscopic projection for representative Group I and Group II species. Different longitudinal and cross-sectional scales are used to permit a single reconstruction to show basal and apical basilar membrane configurations, membrane length (ML), and the proportions of inner and outer laminae.

Thus, in the extreme basal end, the basilar membrane is firmly anchored at both margins to a bony shelf. In Delphinidae, the outer lamina thins, paralleling the inner lamina, and the spiral ligament replaces it as the primary lateral membrane support; an ossified outer shelf is found only in the first 8 to 10 mm of the average delphinid duct (Fig. 8). In Phocoena, bony laminae are present medially and laterally for 17 to 18 mm, ending with no significant taper. The basilar membrane therefore is provided with substantial buttressing at both edges over 60% its length in Phocoena and 20 to 28% of its length in delphinids.

Total ganglion cell counts and ganglion cell densities were estimated for one specimen of Phocoena, Tursiops, and Stenella attenuata from 20 μ serial sections corrected for intersection partial cell duplications (Table 5). Data from human temporal bones, perfused Lagenorhynchus obliquidens, and horseshoe bats are listed for comparison. Normal human temporal bone data are useful comparisons because they have similar preservation hazards as fisheries and stranded animals. Surprisingly, odontocete data from previous studies for perfused animals and data from this study are similar. Ganglion cell densities for all odontocetes are more than twice those of bats and humans. They are also 30-50% greater than the highest densities reported in the basal, foveal regions in bats.

Cochlear Morphometrics and Topology

Most attempts at cochlear spiral measurements use two-dimensional interpolation techniques (Guild, 1921) or serial section plots (Schuknecht, 1953; Wever et al.,1971a). Although these methods provide reasonable approximations of spiral shapes, all orthographic projections have the same inherent disadvantage; i.e., flat plots are necessarily foreshortened. In shadow projections, tall or short spirals with equal interturn radii produce the same axial silhouette and they will appear to have the same length regardless of differences in height (Fig. 9). Useful allometric analyses require all three dimensions be taken into account.

Table 5. Ganglion Cell Density

Species	Total Ganglion Cells	Membrane Length (mm)	Average Density (cells/mm)
Phocoena phocoena	66933	24.31	2753.3
Lagenorhynchus obliquidens	70000[1]	34.90	2005.7
Stenella attenuata	82506	37.68	2189.6
Tursiops truncatus	105043	41.57	2526.9
Rhinolophus ferrumequinum	15953	16.10	1000/1750[2]
Homo sapiens	30500[3]	31.00	983.9

[1]Wever et al.(1972)
[2]Bruns and Schmieszek (1980); cochlear average/acoustic fovea densities.
[3]Schuknecht and Gulya (1986)

Three-dimensional cochlear spiral measurements for key species are compared with ultrasonic frequency ranges in Table 6. There is a strong negative correlation ($-0.968<r<-0.791$) for characteristic frequency and all spiral variables except scalae length and basal diameter, which have a positive correlation with animal length ($0.84<r<0.92$). Principal component analyses distribute the data into two frequency-weighted divisions with 91% of variability attributed to body length and spiral geometry. Excluding frequency, the data redistribute into three categories: short body length and low cochlear spiral parameters (Phocoena); long body length and low parameters (Physeter); and short to average length with

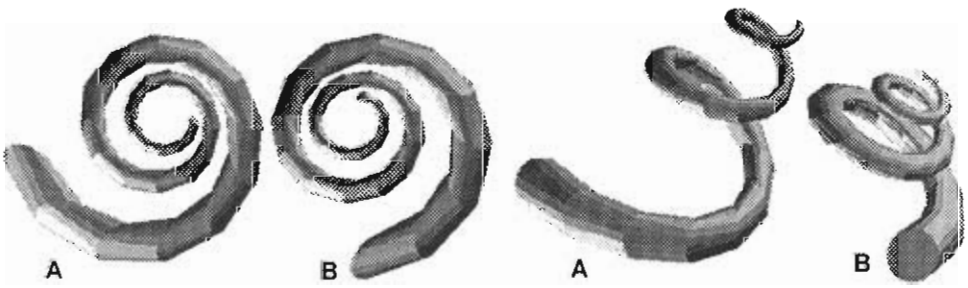

Fig. 9. Orthogonal vs. Three-dimensional Projections. The spiral pair on the right are 70° rotations of the left. An initial pair was generated by computing two spirals in which all variables are constant except vertical increment/rotation and final path length. These were then displayed at two rotations. In axial projections (left), their differences appear negligible and center-line plots of their paths would be indistinguishable. As is apparent in side views, spiral A is actually 15% longer with an axial height 135% that of B.

Table 6. Cochlear Canal Spiral Parameters

Group and Species	Turns	Scalae Length (mm)	Basal Diam. (mm)	Axial Height (mm)	Axial Pitch[1] (mm)	Basal Ratio[2]	Slope Ratio[3]	Echolocation Pulse Peak Frequency (kHz)
I								
Phocoena phocoena	1.5	25.93	5.25	1.47	0.982	0.280	.038	130
Physeter catodon	1.75	72.21	14.3	3.12	1.78	0.218	.025	unknown[5]
Inia geoffrensis[4]	1.5	38.2	8.5	-	-	-	-	200
II								
Grampus griseus	2.5	40.5	8.73	5.35	2.14	0.614	.053	unknown[5]
Lagenorhynchus albirostris	2.5	34.9	8.74	5.28	2.11	0.604	.061	40
Stenella attenuata	2.5	36.9	8.61	4.36	1.75	0.507	.047	60
Tursiops truncatus	2.25	40.65	9.45	5.03	2.24	0.532	.055	70

1 $\frac{\text{axial height}}{\text{turns}}$ 2 $\frac{\text{axial height}}{\text{basal turn diameter}}$ 3 $\frac{[\text{axial height/scalae length}]}{\text{turns}}$

[4] All measurements for Inia are estimates from single plane X-rays.

[5] Echolocation has not been documented in these species.

high spiral parameters (Delphinidae). These data indicate two spiral morphometries, Type I and Type II, differentiated by turns, height, pitch, slope, and basal ratios. Species distributions for Type I and II spirals coincide with acoustic Groups I and II and with differences found in outer osseous laminar configuration. Although T-tests showed no significant differences between Groups I and II for bullar surface variables or standardized scalae length, spiral configuration data for the groups differ with significance levels beyond 0.1%.

Type I and Type II spirals are closely modelled by Archimedian (I) and equiangular (II) spirals (Fig. 10). In ideal forms, these two spirals represent (I) a constant interturn radius curve, like that of a tightly coiled rope, and (II) a gnomonic spiral with logarithmically increasing interturn radii; e.g., a chambered nautilus. The gnomonic spiral is common in nature and is the assumed configuration for mammalian cochlea. The archimedean curve is rare. The mathematical parameters for Type I and Type II are:

I	II
$r = a\theta$	$r = e^{a\theta}$
$N < 2$	$N > 2$
$\left(\frac{r_n}{n}\right) \geq \left(\frac{r_{n+1}}{n+1}\right)$	$\left(\frac{r_n}{n}\right) \leq \left(\frac{r_{n+1}}{n+1}\right)$

where r = total radius at turn n; N = number of turns; θ = angular displacement (radians); and a = a spiral size constant. For odontocete cochlea, a is species-isometric and is calculated retroactively for the models from basal ratios (Figs. 10, 11).

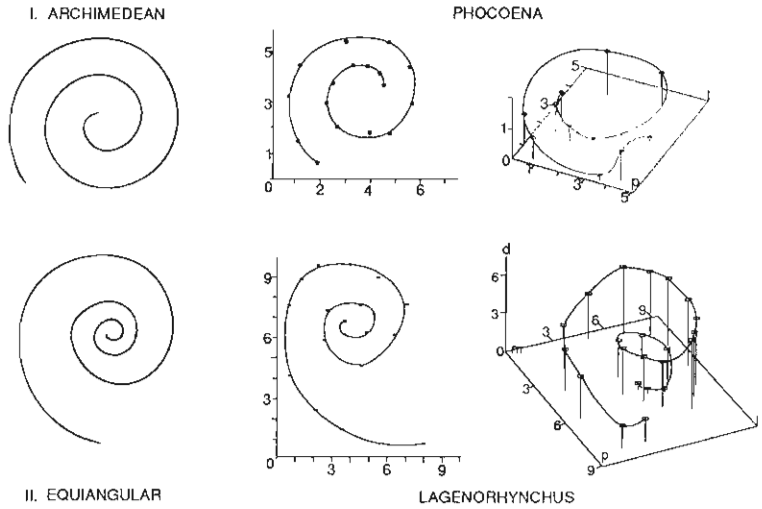

Fig. 10. Spiral Models and Species Cochlear Canal Plots. Ideal Type I and Type II spirals are shown for comparison with plots of cochlear canal midpoints in Phocoena phocoena and Lagenorhynchus albirostris. Two-dimensional projections are based on single-plane X-rays. Three-dimensional plots were obtained from 2 mm. CT scans of the same animal and include the cochlear hook which cannot be seen in a flat, axial image. Flattened contours appear in the three-dimensional curves where all points of a cochlear half-turn fell within one CT scan. Axes are scaled in millimeters. m medial, p posterior, l lateral, d dorsal.

CONCLUSIONS

The principal question posed in this study was whether three-dimensional comparative assessments of the auditory periphery could provide insights into the ability of odontocetes to echolocate in water. Anatomical analyses and three-dimensional reconstructions show a complex peripheral auditory architecture which is unique to odontocetes. Their temporal bone is adapted for both acoustic isolation and for pressures encountered in an aquatic environment, while the inner ear is clearly adapted for ultrasonic perception. Inner ear modifications related to ultrasonic audition found in all odontocetes included an exceptionally narrow basal basilar membrane, high spiral ganglion cell densities, and extensive, bony outer spiral lamina. Moreover, there are two cochlear spiral configurations which correlate with odontocete echolocation signal ranges. These configurations, when combined with species data on cochlear duct laminae distributions, can be used to predict classes of odontocete ultrasonic audition.

Comparisons of odontocete and bat bullae imply that temporal bone structure is strongly influenced by environmental factors. Unlike the fragile,

inflated bullae of bats, all odontocete bullae are constructed of massive, porcelaneous bone which resists compression. Both the middle ear and peribullar cavities are lined with specialized membranes, the corpus cavernosum and peribullar plexus, which are highly vascularized and which may moderate volume changes which would be catastrophic in fully pneumatized cavities. Ligaments replace bony attachments to the skull, providing acoustic isolation. The periotic and tympanic differ in mass, have specific low density regions or windows, and, in some species, are virtually hinged by a flexible tympano-periotic suture, raising possibilities for differential vibration and conduction properties throughout the bulla. Although this study did not directly address alternatives to a tympanic or ossicular path for sound transmission to the cochlea, the position, construction, and ligamentous associations of the bulla support the "pan bone" theory of jaw conduction (Norris, 1969; Norris and Harvey, 1974), and, like facial ruff assymetries in barn owls (Knudsen, 1981), bilateral asymmetries in the location of the bullae may provide directional cues.

All bullae examined in situ were oriented with the periotic medial and dorsal to the tympanic. This orientation results in the cochlear apex ventral to the stapes, orthogonal to the terrestrial mammalian format. This placement, or displacement, of the ear may result from the spinal flexion and caudal brain case compression that occurred in odontocetes as they regressed to a fuselloid shape, but its utilitarian effect is a shorter, less angular pathway for the VIIIth nerve which crosses the peribullar cavity before entering the brain case. This "externalization" of the auditory nerve may be unique in odontocetes. It arises from the separation of the bulla from the skull, which is adaptive for aquatic echolocation, and provides a functional explanation for the dense fibrous sheath fully enclosing the VIIIth nerve.

Basilar membrane length varies with animal size and is not correlated with peak ultrasonic frequency. Membrane widths in this study are smaller than reports by Fleischer (1976) and Norris and Leatherwood (1981). Neither work listed animal lengths, which could account for 10% variability; however, differences in our results may be explained also by technique. Fleischer used a deep corrosive cast and estimated widths from interlaminar gaps. Norris and Leatherwood used an extremely corrosive, rapid decalcificant, trichloracetic acid, on salvaged tissues. Either method will distort or etch bony membrane supports and yield overestimates. The measurements in this study are comparable to those by Wever et al. (1971a; 1972) for perfused Tursiops and Lagenorhynchus.

Basilar membrane dimensions interact with its composition and support to determine resonance characteristics. Based upon dimensions alone, the odontocete membrane is a highly differentiated, anisotropic structure capable of an exceptionally wide frequency response. In the basal end, the basilar membrane in all odontocetes is nearly square with a 400-600μ^2 cross-sectional area and is tightly joined to double laminae. Apically, it thins to a 5μ x 300-450μ strip supported by ligaments. The basal construction is characteristic of echolocators (Hinchcliffe and Pye, 1969), but while bat and odontocete basilar membranes are similar, odontocete basal ratios are substantially greater. Membrane ratios plotted as a percentage of membrane length (Fig. 7) are significantly higher for the basal turn of odontocetes. Were other cochlear duct structures identical, the differences in the ratios, which reflect structural

differences related to membrane stiffness, are sufficient to account for lower ultrasonic ranges in bats.

The diameter of the auditory nerve (Table 3), the volume of habenular nerve fibers in the osseous spiral lamina, and high ganglion cell counts are consistent with hypertrophy of the entire odontocete auditory system. For quantitative interspecific comparisons, ganglion cell density is a more effective measure than total cell population. Densities in this study ranged from 2000 cells/mm in Lagenorhynchus to 2700 cells/mm in Phocoena, which are higher than in any other mammal. Wever et al. (1971b, 1972) reported ganglion:hair cell ratios of 4:1 for Lagenorhynchus and 5:1 for Tursiops. Virtually all mammals average 100 inner hair cells/mm (N. Kiang, pers. comm.) with 2.5 to 4 rows of outer hair cells/inner hair cell. Wever's data imply a hair cell array of 1 inner and 4 outer rows in two odontocetes. Using this estimate with our data, we calculate a nearly 6:1 ratio for Phocoena phocoena, 5:1 for Tursiops truncatus, 4.4:1 for Stenella attenuata, and 4:1 for Lagenorhynchus obliquidens. The human ratio is 2.4; cats, 3; and bats range 3-5:1 (Firbas, 1972, Bruns and Schmieszek, 1980). Since 90-95% of all afferent spiral ganglion cells innervate inner hair cells, we estimate an average ganglion cell:inner hair cell ratio of 24 for odontocetes. This is more than twice the average density in bats and three-fold that of humans (Firbas, 1972). While data from three specimens are insufficient for a definitive analysis, ganglion cell:hair cell ratios appear to be proportional to frequency ranges in both bats and odontocetes and it is likely that higher afferent ratios in odontocetes are directly related to the extent or complexity of information extracted by neuronal processing of their echolocation signals.

The presence of an external bony lamina is virtually diagnostic for ultrasonic perception (Sales and Pye, 1974; Reysenbach de Haan, 1956). Differences in laminar structure amongst odontocetes are consistent with acoustic divisions and provide a simple but important mechanistic link for species differences in ultrasonic ranges. In Odontoceti, the extent of the ossified lateral spiral lamina is a species and group-specific character. Phocoenids have the highest frequency range and a substantial outer lamina over two-thirds of the cochlear duct. Delphinids have a characteristic outer lamina for 20-30% of the duct. Since the basal basilar membrane is similarly constructed in both groups, a longer outer lamina in Group I increases membrane stiffness, thereby increasing the resonant frequency for that membrane region, compared to equivalent, unsupported membrane locations in Group II.

Cochlear spiral measurements show a clear division of odontocete inner ears into two types which correlate with cochlear duct differences in laminae. The divisions are not determined by taxonomy but by complex spiral geometry. Categorizations of species by spiral format also coincide with high and low echolocation frequency groups:

I. Type I species have a nearly planar cochlear spiral with a slope ratio <0.04 and a constant radial increment. Axial height is less than 0.1% body length and the basal ratio ranges 0.2-0.3. There are less than two full turns. Outer spiral laminae buttress the basilar membrane for >60% its length. Peak energy of echolocation clicks for known species is located above 100 kHz.

II. Type II species have a more attenuated spiral with logarithmically increasing radii, an axial height more than 0.2% body length, and slope ratios >0.05. The basal ratio is >0.5. There are typically 2.5 turns with outer bony laminae present 25% of basilar membrane length. Type II species generally produce broad spectrum ultrasonic clicks with peak energy below 100 kHz.

Three-dimensional composite reconstructions graphically demonstrate the configurational differences between Type I and Type II odontocete cochlea (Fig. 11). The composites were produced by combining spiral model parameters, cochlear canal data, and cochlear duct contour measurements of Group I and Group II species. Contours of the basilar membrane, spiral ganglia, and inner and outer laminae were digitized, measured, standardized by animal length, and plotted in a computerized, three-dimensional framework to obtain a weighted average contour for each component. A principal spiral was generated by plotting a Type I or Type II spiral with constants derived from normalized species averages. Regular structures were produced centered on the spiral by superimposing the averaged contours on the spirals at the mid-modiolar plane and interpolating each component along the curve. In both Type I and Type II cochlea, the spiral ganglia are distributed in a continuous band for nearly 80% of cochlear duct length, but differences in cell densities are implied by the smaller volume of the ganglia in the Type II reconstruction Differences in membrane buttressing between types are clear. The Type I cochlea has proportionately twice as much membrane supported by bony laminae as Type II. The basilar membrane, which normally stretches between the inner and outer spiral laminae or spiral ligament, is represented only by its outer edge to avoid blocking views of other structures. At the apex, the Type II membrane is broader, which suggests these species have a wider frequency range than Type I. This is likely to be true for lower frequencies, but differences in basal laminar support imply Type II cochlea have a lower ultrasonic capacity.

Type II spirals resemble the conventional, terrestrial cochlear format and include the delphinid species which have been most extensively investigated in the past. Type I represents a novel cochlear format with major deviations from conventional assumptions of cochlear modelling. The combination of Type I spiral configuration, more extensive laminar buttressing, and higher echolocation frequencies in Group I species argues strongly for an adaptive relationship to aquatic echolocation for this cochlear format. Since the data in this survey for Type I cochlea are dominated by Phocoena phocoena, it could be argued they represent a single, distinctive genus rather than a format for upper range ultrasonic audition. Evidence that there are at least two spiral formats can be adduced, however, from anatomical and behavioural studies in other species.

If we assume echolocation frequencies are correlated habitat, differences in species distributions for Type I and Type II spiral formats should correlate with environmental distributions as well. Fresh water and near shore species live in an information dense, structurally complex environment. Since wavelength is inversely related to frequency, using echolocation to differentiate the small structures typical of these waters requires exceptionally high frequencies. The same range of higher frequencies would be of little use to open ocean species which, by comparison, live in extremely low density environments and are primarily concerned with detection of larger, distant objects or communication

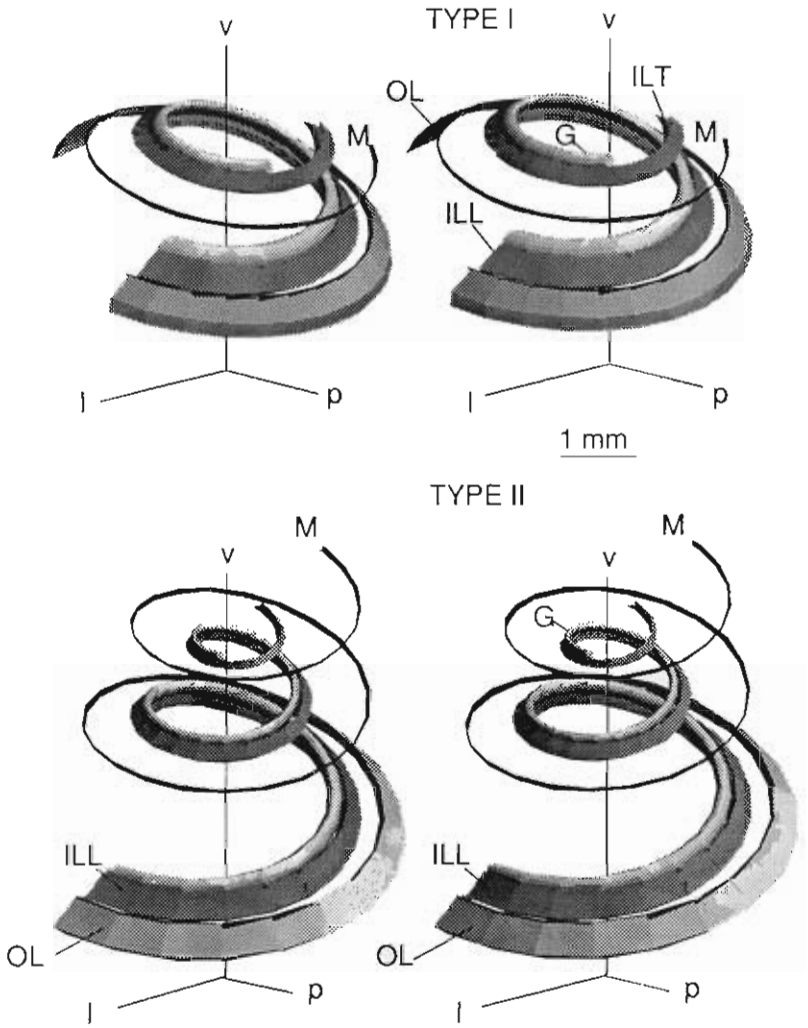

Fig. 11. Basilar Membrane, Spiral Lamina, and Neural Fiber Distributions in Odontocetes. Composite reconstructions, generated from standardized data, schematically represent major cochlear duct structural and neural components of Type I and Type II odontocetes. Principal features are described in the text. The images are reproduced as parallel stereo-pairs with an approximate viewing distance of 25 cm. Most conventional stereo-viewers may also be used. The spirals have been scaled to common axes to facilitate comparisons. The cochlea are inverted, as in Figures 6 and 7, from in vivo orientations. l lateral, p posterior, v ventral; G spiral ganglia; IL inner osseous spiral lamina (L limbal edge; T tympanal); M basilar membrane (lateral edge); OL outer osseous spiral lamina.

with conspecifics. With these assumptions, we would predict platanistid, riverine dolphins living in the Ganges or varzea lakes of the Amazon to be higher frequency, Type I species. In fact, echolocation signals of these species range to 200 kHz and illustrations show cochlea with 1.5 turns (Purves and Pilleri, 1983), consistent with our radiographic evidence for Inia. They fit the Type I format qualitatively and Group I acoustically. A recent study by Feng et al. (1986) shows 1.5 evenly distributed turns in Lipotes, the Chinese river dolphin, as well. These comparisons suggest that Type I spirals are not a unique adaptation of Phocoena. For two key species, Grampus griseus and Physeter catodon, we have no corroborative recordings. Grampus are off-shore animals which travel in pods and anecdotal reports indicate they whistle. The cochlear data for Grampus fall clearly within Type II parameters, implying an echolocation range below 100 kHz. In contrast, Physeter has a Type I format numerically, but there are several additional factors to consider. Unlike the earlier species presumed to be Type I, Physeter is pelagic and it has a substantially different bullar anatomy. There is no evidence to date for echolocation in Physeter. No structural analyses of any physeterid cochlear duct are yet available, but they are imperative for frequency estimates since spiral configuration alone cannot dictate inner ear resonance characteristics, and the immense size of Physeter catodon may radically affect cochlear structure. Our data indicate at least one alternative cochlear configuration exists in odontocetes which is coincident with extensive bony laminae, high basilar membrane ratios, and higher ultrasonic auditory ranges. Physterid cochleae appear, preliminarily, to resemble this format, but they may also represent a third alternative from which we may discover the limits which size alone can impose on the ability of even odontocetes to produce or perceive ultrasonics. While our data begin to reveal the diversity of odontocete cochlea, they impel us also to expand investigations to even more species if we are to understand the true range of the odontocete ear.

ACKNOWLEDGMENTS

This work was supported by the ARCS Foundation and NSF grant BNS-8118072. All specimens were collected under Permit no. 368, National Marine Fisheries Service, National Oceanic and Atmospheric Administration, Department of Commerce, in compliance with the Endangered Species Act and Marine Mammal Protection Act. The work could not have been completed without the encouragement and assistance of the staffs of the Departments of Anatomy, Experimental Radiology, and Neuroradiology of the Johns Hopkins Medical Institutions. Invaluable assistance with radiographic studies were provided by Frank Starr, III, James Anderson, and Arthur Rosenbaum. Alan Walker, Willard Graves, and George Carey provided advice and assistance with reconstructions. Key specimens were obtained through the efforts of Gregory Early, Joseph Geraci, James Gilpatrick, Richard Lammertson, Daniel Odell, William Perrin, James Mead, and Charles Potter. Nelson Kiang and Steven Rauch provided helpful reviews on the manuscript. Final reconstructions and graphics were produced with the cooperation of the Cochlear Implant Research Laboratory, the Eaton-Peabody Laboratory for Auditory Physiology, and the Department of Otolaryngology, Massachusetts Eye and Ear Infirmary.

Abbreviations in figures:

A apex
a anterior
ap petrotympanic aperture
B basal turn of the cochlea
bo basioccipital
C cochlear spiral
d dorsal
G spiral ganglia
Gf habenula perforata
H cells of Huschke
IAM internal auditory meatus
IL lamina spiralis ossea primaria (inner lamina)
l lateral
Li spiral ligament
M basilar membrane
m medial
Ma mandible
ML membrane length
N auditory nerve
OC organ of Corti
OL lamina spiralis ossea secundaria (outer lamina)
OW oval window (fenestra ovalis)
P periotic
p posterior
P_a anterior periotic edge
Pr promontorium
Pv ventral promontorium edge
R Reissner's membrane
SL spiral limbus
SM scala media
Sp spiral prominence
sp sigmoid process
sq squamosal
ST scala tympani
SV scala vestibuli
Sv stria vascularis
T tectorial membrane
Tl lateral tympanic lobe
Tpl lateral posterior tympanic prominence.
Tpm medial posterior tympanic prominence
v ventral

REFERENCES

Au, W.W.L., Floyd, R.W.,Penner, R.H. and Murchison, A.E., 1974, Measurement of echolocation signals of the Atlantic Bottle-nosed dolphin, Tursiops truncatus montagu, in open waters, J. Acoust. Soc. of Am., 56: 1280-1290.

Brownlee, S., 1983, Correlations between Sounds and Behavior in the Hawaiian Spinner Dolphin, Stenella longirostris, M.S. thesis, University of California, Santa Cruz.

Bruns, V., 1976, Peripheral auditory tuning in the Doppler shift compensating bat, Rhinolophus ferrumequinum: II. Frequency mapping in the cochlea, J. Comp. Physiol., 106: 77-86.

Bruns, V. and Schmieszek, E.T., 1980, Cochlear innervation in the greater horseshoe bat: Demonstration of an acoustic fovea, Hearing Res., 3:27-43.

Bullock, T.H., Grinnell, A.D., Ikezono, E., Kameda, K., Katsuki, Y., Nomoto, M., Sato, O., Suga, N., and Yanagisawa., K., 1968, Electrophysiological studies of central auditory mechanisms in cetaceans, Z. vergl. Physiol., 59: 117-156.

Bullock, T., and Ridgway,S., 1972, Evoked potentials in the central auditory system of alert porpoises to their own and artificial sounds, Jour. Neurobiol., 3: 79-99,

Busnel, R-G., and Dziedzic,A., 1966, Acoustic signals of the pilot whale Globicephala melaena and of the porpoises Delphinus delphis and Phocoena phocoena, in: "Whales, Dolphins, and Porpoises," K.S. Norris, ed., University of California Press, Berkeley.

Caldwell, M.C., and Caldwell, D.K., 1967, Intraspecific transfer of information via pulsed sound in captive odontocete cetaceans, in: "Animal Sonar

Systems: Biology and Bionics, II," R-G. Busnel, ed., Laboratoire de Physiologie Acoustique, Jouy-en-Josas.
Caldwell, M.C. and Caldwell, D. K., 1971, Statistical evidence for individual signature whistles in Pacific whitesided dolphins, Lagenorhynchus obliquidens, Cetology, 3: 1-9.
Camhi, J.M., 1984, "Neuroethology: Nerve Cells and the Natural Behavior of Animals," Sinauer Assoc., Inc., Sunderland.
Diercks, K.J., 1972, Biological sonar systems: A bionics survey, Applied Research Laboratories, ARL-TR-72-34, University of Texas.
Diercks, K.J., Trochta, R.T., Greenlaw, R.L., and Evans, W.E., 1971, Recording and analysis of dolphin echolocation signals, J. Acoust. Soc. Am., 49: 1729-1732.
Evans, W.E., 1967, Vocalizations among marine mammals, in: "Marine Bio-Acoustics," W.N. Tavolga, ed., Pergamon, New York.
Evans, W.E., 1973, Echolocation by marine delphinids and one species of fresh water dolphin, J. Acoust. Soc. Am. , 54: 191-199.
Evans, W.E., and Prescott, J.H., 1962, Observations of the sound production capabilities of the bottlenose porpoise: A study of whistles and clicks, Zoologica, 47: 121-128.
Feng, W., Liang, C, Wang, J., and Wang,X., 1986, Morphometric and Stereoscopic Studies on the Spiral and Vestibular Ganglia of Lipotes vexillifer,, (prepubl.).
Firbas, W., 1972, Über anatomische Anpassungen des Hörorgans an die Aufnahme hoher Frequenzen, Monatsschr. Ohr. Laryn.-Rhinol., 106:105-156
Fleischer, G., 1976, Hearing in extinct cetaceans as determined by cochlear structure, Jour. Paleon., 50: 133-152.
Fraser, F., and Purves.,P., 1960, Hearing in cetaceans: Evolution of the accessory air sacs in the structure and function of the outer and middle ear in Recent cetaceans, Bull. Brit. Mus. Nat. Hist., 7: 1-140.
Graves, W.L., Carey, G.A., Benac, S.L., and Cameron, L.W., 1984, Modeling and Graphic Display System for Cardiovascular Research Using Random 3-D Data, IEEE 1984 Int. Symp. on Medical Images and Icons, 304-308.
Grinnell, A.D., 1963, The neurophysiology of audition in bats: Intensity and frequency parameters, J. Physiol., 167: 38-66.
Guild, S.R., 1921, A graphic reconstruction method for the study of the organ of Corti, Anat. Rec., 22: 141-157.
Hinchcliffe, R., and Pye.,A, 1968, The cochlea in Chiroptera: A quantitative approach, Int. Audiol., 7: 259-266.
Hinchcliffe, R., and Pye., A., 1969, Variations in the middle ear of the Mammalia, J. Zool., 157: 277-288.
Iurato, S., 1962, Functional implications of the nature and submicroscopic structure of tectorial and basilar membranes, J. Acoust. Soc. of Am., 34: 1368-1395.
Kamminga, C.F., Engelsma, F.J., and Terry, R.P., 1989, Acoustic observations and comparison on wild, captive and open water Sotalia and Inia, Eighth Bienn. Conf. Biol. Mar. Mamm., 33.
Kasuya, T., 1973, Systematic consideration of recent toothed whales based on the morphology of tympano-periotic bone, Sci. Rep. Whale Res. Inst., 25: 1-103.
Kellogg, W.N., 1959, Auditory perception of submerged objects by porpoises, J. Acoust. Soc. Am., 31: 1-6.

Ketten, D.R., 1984, Correlations of Morphology with Frequency for Odontocete Cochlea: Systematics and Topology, Ph.D. thesis, The Johns Hopkins University, Baltimore.

Knudsen, E.I., 1981, The Hearing of the barn owl, Sci Am., 245(6): 113-125.

Long, G.R., 1980, Some psychophysical measurements of frequency in the greater horseshoe bat, in: "Psychophysical, Psychological, and Behavioural Studies in Hearing," G. van den Brink and F. Bilsen, eds., Delft University Press, Delft.

Maue-Dickson, W., Dickson, D.R., and Pullen, F.W., 1983, "Computed Tomographic Atlas of the Head and Neck," Little, Brown and Co., New York.

McCormick, J.G., Weaver, E.G., Palin, G., and Ridgway, S.H., 1970, Sound conduction in the dolphin ear, J. Acoust. Soc. Am., 48: 1418-1428.

Møhl, B., and Andersen, S., 1973, Echolocation: High-frequency component in the click of the harbor porpoise (Phocoena phocoena L.), J. Acoust. Soc. Am., 57: 1368-1372.

Montali, R.J., and Migaki, G., 1980, "The Comparative Pathology of Zoo Animals," Smithsonian Inst. Press, Wash., D.C.

Moore, P.W.B., 1990, Investigations on the control of echolocation pulses in the dolphin, (this volume).

Moran, P.R., Nickles, R.J., and Zagzebski, J.A., 1983, The physics of medical imaging, Phys. Today, July: 36-42.

Nagel, E.L., Morgane, P.J., and McFarland, W.L., 1964, Anesthesia for the bottlenose dolphin, Tursiops truncatus, Science, 146: 1591-1593.

Neuweiler, G., 1980, Auditory processing of echoes: Peripheral processing, in: "Animal Sonar Systems," R-G Busnel and J.F. Fish, eds., Plenum Press, New York.

Norris, J., and Leatherwood, K., 1981, Hearing in the Bowhead Whale, Balaena mysticetus, as estimated by cochlear morphology, Hubbs Sea World Rsch. Inst. Tech. Rpt. no. 81-132: 15.1-15.49.

Norris, K.S., 1969, The echolocation of marine mammals, in: "The Biology of Marine Mammals," H.J. Andersen, ed., Academic Press, New York.

Norris, K.S., and Harvey., G.W., 1974, Sound transmission in the porpoise head, J. Acoust. Soc. Am., 56: 659-664.

Norris , K.S., Harvey, G.W., Burzell, L.A., and Krishna Kartha, D.K., 1972, Sound production in the freshwater porpoise Sotalia cf. fluviatilis Gervais and Deville and Inia geoffrensis Blainville in the Rio Negro Brazil, in: "Investigations on Cetacea," G. Pilleri, ed., 4: 251-262, University of Berne, Berne.

Norris, K.S., Prescott, J.H., Asa-Dorian, P.V., and Perkins., P., 1961, An experimental demonstration of echolocation behavior in the porpoise, Tursiops truncatus, Montagu, Biol. Bull., 120: 163-176.

Oelschlager, H. A., 1990, Evolutionary morphology and acoustics in the dolphin skull, (this volume).

Oelschlager, H. A., 1986, Comparative morphology and evolution of the otic region in toothed whales, Am J. Anat., 177: 353-368.

Pilleri, G., 1983, The sonar system of the dolphins, Endeavour, 7: 59-64.

Pollack, G.D., 1980, Organizational and encoding features of single neurons in the inferior colliculus of bats, in: "Animal Sonar Systems," R-G Busnel and J.F. Fish, eds., Plenum Press, New York.

Popper, A.N., 1980, Sound emission and detection by delphinids, in: "Cetacean Behavior: Mechanisms and Functions," L.M. Herman, ed., John Wiley and Sons, New York.
Purves, P.E., and Pilleri, G.E., 1983, "Echolocation in Whales and Dolphins," Academic Press, Inc., Ltd., London.
Reysenbach de Haan, F.W., 1956, Hearing in whales, Acta Otolaryngol., Suppl., 134: 1-114.
Ridgway, S.H., 1980, Electrophysiological experiments on hearing in odontocetes, in: "Animal Sonar Systems," R-G. Busnel and J.F. Fish, eds., Plenum Press, New York.
Ridgway, S.H., and McCormick., J.G., 1967, Anesthetization of porpoises for major surgery, Science, 158: 510-512.
Ridgway, S.H., McCormick, J.G., and Wever, E.G., 1974, Surgical approach to the dolphin's ear, J. Expl. Zool., 188: 265-276.
Sales, G., and Pye, D., 1974, "Ultrasonic Communication by Animals," John Wiley and Sons, New York.
Schevill, W. E., 1964, Underwater sounds of cetaceans, in: "Marine Bio-Acoustics," W.N. Tavolga, ed., Pergamon Press, New York.
Schuknecht, H.F., 1953, Technique for study of cochlear function and pathology in experimental animals, Arch. Otolaryngol., 58: 377-397.
Schuknecht, H.F., and Gulya, A.J., 1986, Anatomy of the Temporal Bone with Surgical Implications. Lea and Feibiger, Philadelphia.
Stinson, M.R., 1983, Implication of ear canal geometry for various acoustical measurements, J. Acoust. Soc. Am., 74(S1): 8.
Suga, N., 1983, Neural representation of bisonar (sic) information in the auditory cortex of the mustached bat, J. Acoust. Soc. Am., 74(S1): 31.
Supin, A.Y. and Popov, V.V., 1990, Frequency selectivity of the auditory system of the bottlenosed dolphin Tursiops truncatus, (this volume).
Thomas, J., Chun, N., and Au, W., 1988, Underwater audiogram of a false killer whale (Pseudorca crassidens), J. Acoust. Soc. Am., 84: 936-940.
Watkins, W., and Schevill, W., 1977, Sperm whale codas, J. Acoust. Soc. Am., 62: 1485-1590.
Watkins, W.A., and Wartzok, D., 1985, Sensory biophysics of marine mammals, Mar. Mamm. Sci., 3: 219-230.
West, C. D., 1986, Cochlear length, spiral turns and hearing, 12th International Congress on Acoustics, 1: B-1.
Wever, E.G., McCormick, J.G., Palin, H., and Ridgway, S., 1971a, The cochlea of the dolphin, Tursiops truncatus: The basilar membrane, Proc. Nat. Acad, Sci., U.S.A., 68: 2708-2711.
Wever, E.G., McCormick, J.G., Palin, H., and Ridgway, S., 1971b, The cochlea of the dolphin, Tursiops truncatus: Hair cells and ganglion cells, Proc, Nat. Acad. Sci., U.S.A., 68: 2908-2912.
Wever, E.G., McCormick, J.G., Palin, H., and Ridgway, S., 1972, Cochlear structure in the dolphin, Lagenorhynchus obliquidens, Proc. Nat. Acad. Sci., U.S.A., 69: 657-661.
Wood, F.G., and Evans, W.E., 1980, Adaptiveness and ecology of echolocation in toothed whales, in: "Animal Sonar Systems," R-G Busnel and J.F. Fish, eds., Plenum Press, New York.
Zwislocki, J., 1981, Sound analyses in the ear: A history of discoveries, Amer. Sci., 69: 184-192.